Chaos, Solitons and Fractals 81 (2015) 184–196

Contents lists available at ScienceDirect

Chaos, Solitons and Fractals

Nonlinear Science, and Nonequilibrium and Complex Phenomena

journal homepage: www.elsevier.com/locate/chaos

Low dimensional chaotic models for the plague epidemic in Bombay (1896–1911)

Sylvain Mangiarotti[1,*]

CESBIO, Centre d'Études Spatiales de la Biosphère,18 av. Edouard Belin, Toulouse 31401, France

ARTICLE INFO

Article history:
Received 3 June 2015
Accepted 12 September 2015

MSC:
Chaos in Bombay plague epidemic

Keywords:
Chaotic system
Global modeling
Epizootic
Plague
Rats
Fleas

ABSTRACT

A plague epidemic broke out in Bombay in 1896 and became endemic. From 1905 to 1911, the epidemic was closely monitored by an Advisory Committee appointed to investigate the causes of the disease in any way. An impressive quantity of information was gathered, analyzed and published. Published data include records of the number of people who died from plague, and of the two main populations of rodents which were infected by plague in Bombay city.

In the present paper, these data are revisited using a global modeling technique. This technique is applied to both single and multivariate observational time series. Several models are obtained for which a chaotic behavior can be observed. Obtaining such models proves that the dynamics of plague can be approximated by low-dimensional deterministic systems that can produce chaos. The multivariate models give a strong argument for interactive couplings between the epidemic and the epizootics of the two main species of rat. An interpretation of this coupling is given.

1. Introduction

Plague is a zoonoses that has already caused several historical pandemics. It has reappeared in several countries during the 1990s as a reemerging disease [1]. Plague is caused by the bacillus *Yersinia Pestis*, discovered in 1894 [2]. Bubonic plague is the most common form of plague. Clinically, bubonic plague is characterized by buboes that result from the infection of lymph nodes. Contrarily to pneumonic plague, which is a severe type of lung infection, bubonic plague is generally transmitted to people by the bite of a flea having transited onto a rat or another rodent infected by the disease and is not transmitted directly from person to person. Without adapted antibiotics, the disease can become septicemic and then lead to the death in the first 36 h, or even less. Plague zoonose may have different specificities from one source of plague to another, however, its dynamics always implies mammal hosts as reservoirs and fleas as vectors. Although the reservoirs, vectors and the main processes at work in the propagation of the disease are well identified, the persistence of this highly virulent disease remains poorly understood.

Since the first model introduced by Kermack and McKendrick in 1927 [3], most of the models for bubonic plague were focused onto the human aspect of the disease. Such models are based on the assumption that the number of cases can be simulated by models made of three compartments corresponding to the susceptible people x, the infected people y and the dead (or immune) people z respectively [3,4]. It was only recently that a plague model taking into

* Tel.: +33561556658; fax: +33561558500.
E-mail address: sylvain.mangiarotti@ird.fr, sylvain.mangiarotti@cesbio.cnes.fr
URL: http://www.cesbio.ups-tlse.fr

[1] Since 2009

http://dx.doi.org/10.1016/j.chaos.2015.09.014
0960-0779/

account interactions between rat and flea populations was attempted [5–7]. Higher-dimensional models resulted from this approach. It is generally assumed in these recent models that the rat epizootic drives the epidemic, so that human cases can be modeled as a by-product of the progression of the disease in the rodent community; such an assumption allows notable simplifications. It is generally also assumed in such models that one single specie of rodent and one single specie of flea are enough to simulate plague progression.

However, it is also known that numerous species of rodents and fleas may carry the plague [8,9]. Black rat (*Mus rattus*) was identified in numerous cases as having a key role in plague epidemic (*e.g.* [10]), but other species of rat [9,11] and other rodents such as marmots, prairie dogs, gerbils, squirrels etc. are also known to be reservoirs of plague [8,12–14]. Moreover, it was observed that epizootics of different species may exhibit differences in their dynamical behavior; It was the case in the Bombay plague, for which a systematic delay in the epizootics of rats *Mus decumanus* and *Mus rattus* was observed [11] (p. 754). It was also found in some places that the immune response to infection may differ within the same endemic area, even for the same specie of rat [10]. Indeed, it was observed in Madagascar that, despite the undeniable susceptibility of rats to plague, populations of very resistant *M. rattus* and *M. norvegicus* could be found in Antananarivo city within the plague-endemic areas [15]. The effective interactions between the population dynamics of the different species in a same source of plague, as well as the relations between susceptible and resistant behaviors remain poorly understood.

It was observed at different geographical places in the world that the populations of different species of flea may exhibit different behaviors in relation to epizootics and epidemic [16,17]. In particular, it was found that some species of flea disliked biting man. However, it was shown that rat-fleas, which do not attack man under normal conditions, may attack once their natural hosts have died off [18]. Fortunately, from a modeling point of view, it was shown that the population of infected flea can be approximated by a stationary state due to the short average time required for a free-living flea to find a new host [7].

Historically, most of the epidemic models are analytically built based on an empirical knowledge of the processes at work. This is in particular the case for Kermack and McKendrick's model for plague. For this reason, as pointed out by its authors, a close fit between the model to the data cannot be expected [3]. Contrary to this, models based on selection techniques are directly obtained from the data and do not require strong *a priori* hypotheses, allowing for a better agreement between model and observational data. Nevertheless, data based approaches generally do not allow to explicit in a comprehensive way the interaction between the variables of the obtained model. A description of the underlying processes remains hard to provide.

In the present work, the Bombay plague epidemic is investigated as case study in order to investigate the possibility (1) to detect chaos from observed plague epidemic, that is, to provide arguments for both determinism and high sensitiveness to initial conditions, and (2) to identify the dynamical couplings existing between the infected people and the two rat epizootics.

The theory of nonlinear dynamical system is used as a background to investigate the problem. The global modeling technique provides deterministic dynamical models that reproduce the trajectory reconstructed from the observational time series. Two types of reconstructed space are mainly used for global modeling, either spanned by derivative coordinates leading to Ordinary Differential Equations [19] or by delay coordinates leading to difference equations [20,21]. In the present work, only the former formulation based on derivative coordinates is considered. Since its earlier applications [19,22], the global modeling technique mostly focused on modeling dynamical behaviors from a single scalar time series. During the last decade, the technique has proved to have the potential to deal with single observable from real world in quite various domains [23–26]. To the best of our knowledge, although several models were obtained from single time series, no dynamical system of Ordinary Differential Equations (that is numerically integrable) was ever obtained directly from multivariate observational data.

In the present paper, it is first attempted to obtain a global model from the multivariate time series collected during the Bombay plague epidemics. The obtained models are then used to explain the so determined couplings between the plague epidemic and the two epizootics of *M. rattus* and *M. decumanus* species. Model validation is based on predictability considerations.

The paper is constructed as follows: Context and data are presented in Section 2. The theoretical background and the methods are described in Section 3. Results are presented in Section 4 where univariate and multivariate models are first considered separately and then compared based on their forecasting ability. The algebraic structure of the multivariate models is then discussed in Section 5. Conclusions are drawn in Section 6.

2. Context and data

2.1. Context

The information that bubonic plague epidemic broke out in Bombay (now Mumbai) in 1896 was first reported by the *British Medical Journal* on October 3rd [27]. The outbreak was estimated *a posteriori* to have taken place in the month of August 1896. December 1896 was marked by a sudden rise of mortality that triggered the alarm; A first Plague Committee for the City of Bombay was appointed by the Bombay Government on the 2nd of March 1897 with the aim to stamp out the disease before the beginning of rains [28]. Once a peak of mortality was reached in January 1897, the mortality progressively decreased, but the epidemic became endemic and propagated year to year without stopping, exhibiting a marked seasonal signal in the mortality.

The first Indian Committees clearly considered the role of rat as a key element but disregarded the flea. The possibility for flea to transmit plague disease from rat to rat was first mentioned by Ogata in 1897 [29] and a first demonstration of its possible role as a vector was given by Simond in 1898 [30]. Probably due to the multiplicity and to the complexity of the situations met, this idea was not immediately accepted

by the international community, despite first confirmations were given in several other works [18,31,32].

After it entered Bombay in 1896, bubonic plague spread throughout all India [33]. It is estimated that in 1904, most of India had been hit by plague [34]. A new Advisory Committee was appointed in 1905 by the *Secretary of State for India*, the *Royal Society* and the *Lister Institute*. It started to explore plague disease in all possible directions. This committee set up in Bombay. Numerous laboratory experiments were then carried out onto rats and fleas to investigate their role in the transmission of plague disease, from rat to rat and from rat to man. Contaminated areas were systematically visited, analyzed, cleaned and disinfected [11] (*e.g.* p. 733, 735). Extensive field investigations were also made to monitor the plague epidemic in the city by gathering all possible information from the beginning of 1905 to the end of 1911 with the help of the Health Department of Bombay City [11] (p. 725; 728–734). A specific monitoring of the epizootics was also performed [11] (p. 735–762). In particular, rodent traps were installed in all the city's quarters in order to get a continuous sampling of the populations of infected rats. A considerable part of the data and analyzes performed by this Advisory Committee was published in the *Journal of Hygiene* since 1906 concerning the period 1896–1911 [11,35–37].

The data analyzes for the period 1896–1911 led the Advisory Committee to several important conclusions. A systematic delay was found between the epizootics of the two main species of rats (*Mus decumanus* and *Mus rattus*) whose populations were tremendous; a delay was also found between the epizootics and the epidemic of Bubonic plague. These studies led the experts to the conclusions that [11]: (1) the epizootic of *M. decumanus* is directly responsible for the diffusion of plague in Bombay city; (2) the epizootic of *M. rattus* is the direct result of the epizootic of *M. decumanus*; (3) the epidemic is the direct result of the epizootic of *M. rattus*, although infection may occasionally be transfered directly from specie *M. decumanus* to human, without the intervention of *M. rattus*.

After this period of sustained monitoring, the mortality due to plague epidemic substantially decreased after 1906, probably thanks to the recommendations of the Advisory Committee. However, plague remained rampant probably much later in all India, at least until the 1920s [38,39]. High peaks of mortality due to plague were again observed in the 1950s. Unfortunately, not so many data were available for the period after 1911.

2.2. Data

Two types of observable are considered in the present work. (1) The first one is the number of human death caused by plague from September 1896 to December 1911. For the earlier months (from September to December 1896), the weekly data were taken from [40]. For the period 1897–1906, data were digitalized from the chart I published with a bimonthly sampling resolution in [35]. This curve being provided as a percentage (see [35], p. 267), a renormalization was performed based on the annual estimates of death due to plague [41]. For the period 1907–1911, the bimonthly data were directly provided as Tables in [36]. The original data of plague death and its resampling at a 4-month time sampling are shown in Fig. 1. The yearly averaged values of plague death per half-month are also reported that clearly show that the epidemic was especially virulent during the period 1897–1906 and became relatively moderate later on.

(2) The second type of data concerns the epizootic of rats. The number of infected rats of the two main species *Mus Decumanus* and *Mus rattus* was monitored by the Advisory Committee from January 1907 to December 1911 [36]. Basically, rodents were daily caught by traps. These were identified (as *M. Decumanus, M. rattus* or others), examined and then classified as infected or not. A bimonthly sampling of these counts is available in [36]. The total number of rodents in Bombay city was impossible to estimate precisely due to their prodigious number, and to their capacity to needle in inaccessible places. To get an idea, note that near 100,000 rats were examined each year from 1906 to 1911 ([11] p. 750, [36]). In the present work, it is assumed that the number of trapped infected rats is a good proxy of the dynamics of total infected rats for each of the two species. The separate counts of the two main species of rats is justified by practical observations, first, by the existence of a time delay (about 10 days [11] p. 754) systematically observed between the dynamics of the two epizootics; second, by the observation of quite different habits of life between the two species. Indeed, *M. rattus* is a house rat, almost domesticated, that lives in close association with man [11] (p. 746, 766). It can be found at any level of a building. It is mostly a grain-eating rat and its nest is commonly found inside houses. *M. Decumanus* is a rat that lives for the most part outside houses. It is mostly found in sewers, storm-water drains, stables, etc. [11] (p. 747). Its nest is found in burrows. Although mostly leaving outside houses, *M. Decumanus* can however not infrequently be found in the lower levels of inhabited buildings (p. 761). Although the two species have specific preferences and habits, they can be both found in places close to foodshops, food godowns, stables, inhabited buildings, etc. [11] (p. 775).

The original records of human mortality due to plague are shown in Fig. 2a together with the records of number of captured infected rats plotted in Fig. 2b and c for the period 1907–1911. For each record, the time series was resampled with a four-month sampling time after which a Savitzky-Golay [42] filter was applied with a $\pm$ 3 weeks window (also superimposed in plain lines to the original records) to calculate the successive time derivatives.

3. Global modeling technique

3.1. Univariate modeling

The global modeling technique aims to obtain deterministic models directly from observational records [19,43]. When applied to single variable, this technique aims to obtain a set of Ordinary Differential Equations in the canonical form

$$\begin{cases} \dot{X}_1 = X_2 \\ \dot{X}_2 = X_3 \\ \vdots \\ \dot{X}_n = F(X_1, X_2, \ldots, X_n), \end{cases} \tag{1}$$

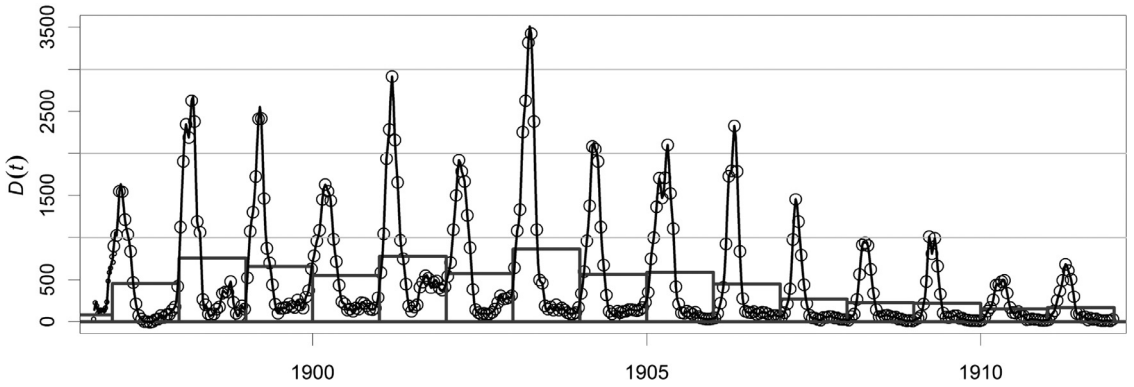

Fig. 1. Number of plague death per half-month from September 1896 to December 1911, in Bombay city. The original data (circles) are bimonthly data [35,36] with the exception of the earlier fifteen values (small dots) which are weekly data [40]. These original records have been resampled at a 4-month time sampling (solid line). Yearly averaged numbers of plague death per half-month are also reported as bars.

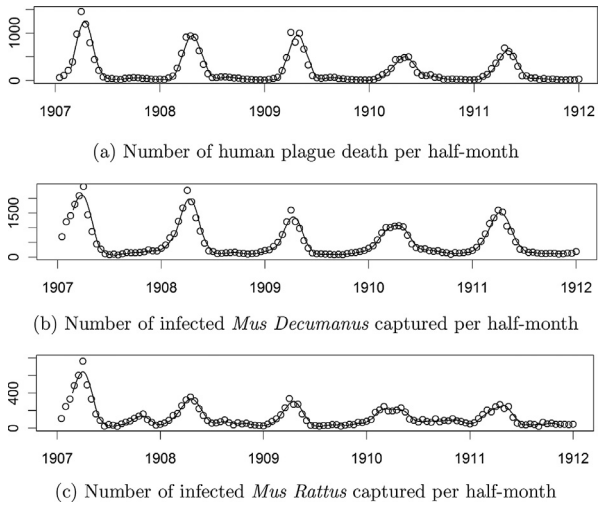

Fig. 2. Time series of the number of human plague deaths per half-month (a) and the number of captured infected *M. Decumanus* (b) and *M. Rattus* (c) per half month, for Bombay city from January 1907 to December 1911 [36]. Original records (circles) have a bimonthly sampling, Filtered curves (plain lines) have been resampled with a four-month sampling time.

where X_1 is the observed variable, and X_2 to X_n its successive derivatives. In practice, the technique consists in retrieving the function $F(X_1, X_2, \ldots, X_n)$ or an approximation of this function. Note that, to be considered as acceptable, a model must – at least – be numerically integrable during a significantly long duration (that is, typically, long enough to get a characteristic Poincaré section) and allow non trivial solutions once transient regime is removed.

Two algorithms (*Polynomial Model Search* and *Global Modeling*) were specifically developed for this purpose; they were tested with theoretical and experimental cases of various difficulty [43]. This algorithm was also applied to environmental data [25,26]. The dimension of the model being *a priori* unknown, the algorithms are successively applied in dimension three, four, etc. In the present case, only three-dimensional models were obtained.

3.2. Multivariate modeling

When several observational records are available, the problem consists in finding a coupling model between the measured variables. When n variables are available, the model form

$$\begin{cases} \dot{x}_1 = f_1(x_1, x_2, \ldots, x_n) \\ \dot{x}_2 = f_2(x_1, x_2, \ldots, x_n) \\ \vdots \\ \dot{x}_n = f_n(x_1, x_2, \ldots, x_n), \end{cases} \tag{2}$$

where functions f_i are approximated by polynomials, can be expected. The multivariate problem thus consists of retrieving a set of n polynomial equations instead of a single one as in Eq. (1). Technically, univariate and multivariate modeling lead to cope with different types of difficulty. Indeed, univariate modeling is intrinsically coherent in its formulation since the formulation of the $(n-1)$ first equations of system (1), that is, the $\dot{X}_i = X_{i+1}$, is built in agreement with the data derivation preprocessing. The difficulty thus focuses onto the single equation: $\dot{X}_n = F(X_1, X_2, \ldots, X_n)$, that is, the last equation of system (1). Contrary to this, the multivariate model (2) does not guarantee *a priori* a consistency. Indeed, because of the (nonlinear) couplings between the equations, each equation will depend on the others. Here, the consistency has to be entirely retrieved. The main difficulty is thus to obtain a numerically integrable set of coupled equations with non-trivial solution in a context where each variable may have an influence onto the others. In that sense, the multivariate modeling is far to be trivial. This is why such type of equations could not be directly obtained from observational data.

In practice, the following steps are applied: First, a set of possible equations $\dot{x}_i = f_i(x_1, x_2, \ldots, x_n)$ is searched for each variable x_i (a polynomial form is used; no structure is predefined: polynomials are selected and constrained automatically). Then, all possible combinations of equations are established for which numerical integrability is tested one by one. Non integrable models are directly rejected. Only the most concise models (12 parameters or less) are considered here. Note that hybrid models combining systems (1) and (2)

Table 1
Window reference (B or C); dates for which univariate U_i and multivariate M_i models were obtained. The various model characteristics are also reported: number N_p of parameter, the polynomial maximum degree q and horizon of predictability H_P (in day, see Section 4.3 for details). H_P values corresponding to the "tuned versions" U_i^t and M_i^t of the models are given in brackets. These latter models were obtained by tuning one model parameter manually until a chaotic dynamic could be reached.

Models	Window	Dates	N_p	Degree q	$H_{P=75\%}$
U_1	(B)	1897–1906	8+2	3	7
U_2	(B)	1899–1907	11+2	3	7 (8)
U_3	(B)	"	16+2	3	7
U_4	(C)	1907–1911	11+2	3	7
M_0	(C)	1907–1911	10	2	31 (20)
M_1	(C)	"	11	2	31
M_2	(C)	"	11	2	31 (29)
M_3	(C)	"	12	2	30 (30)
M_4	(C)	"	12	2	28 (29)

were also investigated, but none of them was integrable in the present analysis.

4. Results

4.1. Univariate modeling

Univariate global modeling was first applied to the record of plague death presented in Fig. 1. No global model could be obtained for the complete time series (August 1896 to December 1911). Three different windows among the available data were thus considered: (A) The earlier period (1896–1897) corresponding to the first epidemic seasonal cycle during which human actions for reducing the spread of the disease was most likely poorly effective due to the sudden appearance and the dramatic progression of the disease; (B) The intermediate period (1897–1905) during which the role of rat fleas was not yet fully accepted by the scientific community and disregarded by the first plague commissions; (C) The last period (1906–1911) during which important efforts were made by the Advisory Committee to take the role of rat fleas into account with the aim to stop the spread of the disease.

No global model was obtained when the first window A (1896–1897) was considered in the analysis. Three models were obtained for the intermediate window B (see Fig. 3, raws 1–3) and one model for the last window C (Fig. 3, last raw). All obtained models are low-dimensional ($n = 3$) and based on polynomials of degree $q = 3$. A general description of the obtained models is given in Table 1 (the detailed formulation of the model polynomials is provided in Appendix A and their initial conditions in Table A.1). The limit expected between the windows B and C was found difficult to detect clearly, most likely because practices applied by the new Advisory Committee during the last window C to curb the epidemic could be implemented only step by step. Important investigations were required to get a clear picture of the situation and actions resulting from these investigations required some delay to become effective and efficient. Anyway, it was clearly observed that no model could be obtained for the entire window B+C. This is interpreted as resulting from a bifurcation or an evolution that occurred between these two windows whereas the behavior remained nearly stationary during each window (B and C) taken individually.

Model U_1 was obtained for window B. This model is a very concise 10-term model (8 terms in the polynomial function +2) that exhibits a weakly developed chaos with a rather simple structure, as shown by the unimodal first-return map to a Poincaré section (Fig. 3, last column). The maximum amplitudes of the model variables (Fig. 3, 2nd column) are in the range of the observations (first column), that is between 0 and 3300 deaths per half-month. It can be noted from the phase portrait that, depending on the number of death people at the earlier beginning of an oscillation, the next oscillation peak may either not exceed 1700 deaths per half-month or reach magnitudes higher than 3000 deaths per half-month.

The univariate model U_2 is a 13-term model obtained from window (1899–1907). This window is mostly focused on B but also includes the earlier beginning of window C (during which the action of the new Advisory Committee remained moderately efficient). This model initially produced a period-4 limit cycle. A fully developed chaos was easily obtained by tuning its parameter values (see Eq. (A.2) in Appendix A). The first return map of the tuned model U_2^t is characterized by three main branches. The amplitude of this second model does not exceed 1700 deaths per half-month (that is corresponding to the smaller oscillations observed in model U_1).

Model U_3 was obtained for the same window as model U_2. It produces a rather complex chaotic attractor (Fig. 3c). Interestingly, its dynamics covers a large range of magnitude from 0 to almost 4000 deaths per half-month which is significantly larger than the observed data whose amplitudes do not exceed 3500. It is important to point out that the possibility to obtain models with larger magnitudes than these actually observed are theoretically explained (indeed, fully developed dynamics may be practically retrieved from a single unstable periodic orbit [44]).

Only model U_4 was obtained for window C. This is a 13-term model that produces a weakly developed chaos characterized by a unimodal first-return map. Amplitudes of the oscillations do not exceed 1000 deaths per half-month as observed during window C. The resulting model suggests that peaks of mortality may not exceed 1000 deaths per half-month during this later window, thus evidencing the effect of the actions performed by this Committee.

These four univariate models provide a strong argument for a low-dimensional deterministic dynamics underlying the epidemic of bubonic plague in Bombay. The detection of these models suggests that the time evolution is strongly controlled by main deterministic processes governing the dynamics. This determinism contributes to explain the difficulty to control the propagation of the disease. At the same time, the analysis shows that plague dynamics is chaotic or very close to chaos which explains the high variability of the signal observed from one year to another, and its weak predictability. It can be noted that the flow of trajectories is especially dense where new oscillations begin. This suggests that the initial conditions, at the beginning of each seasonal oscillation, will have an important influence on the next oscillation peak; and, that a preventive action may have a stronger impact during the earlier development of each epidemic

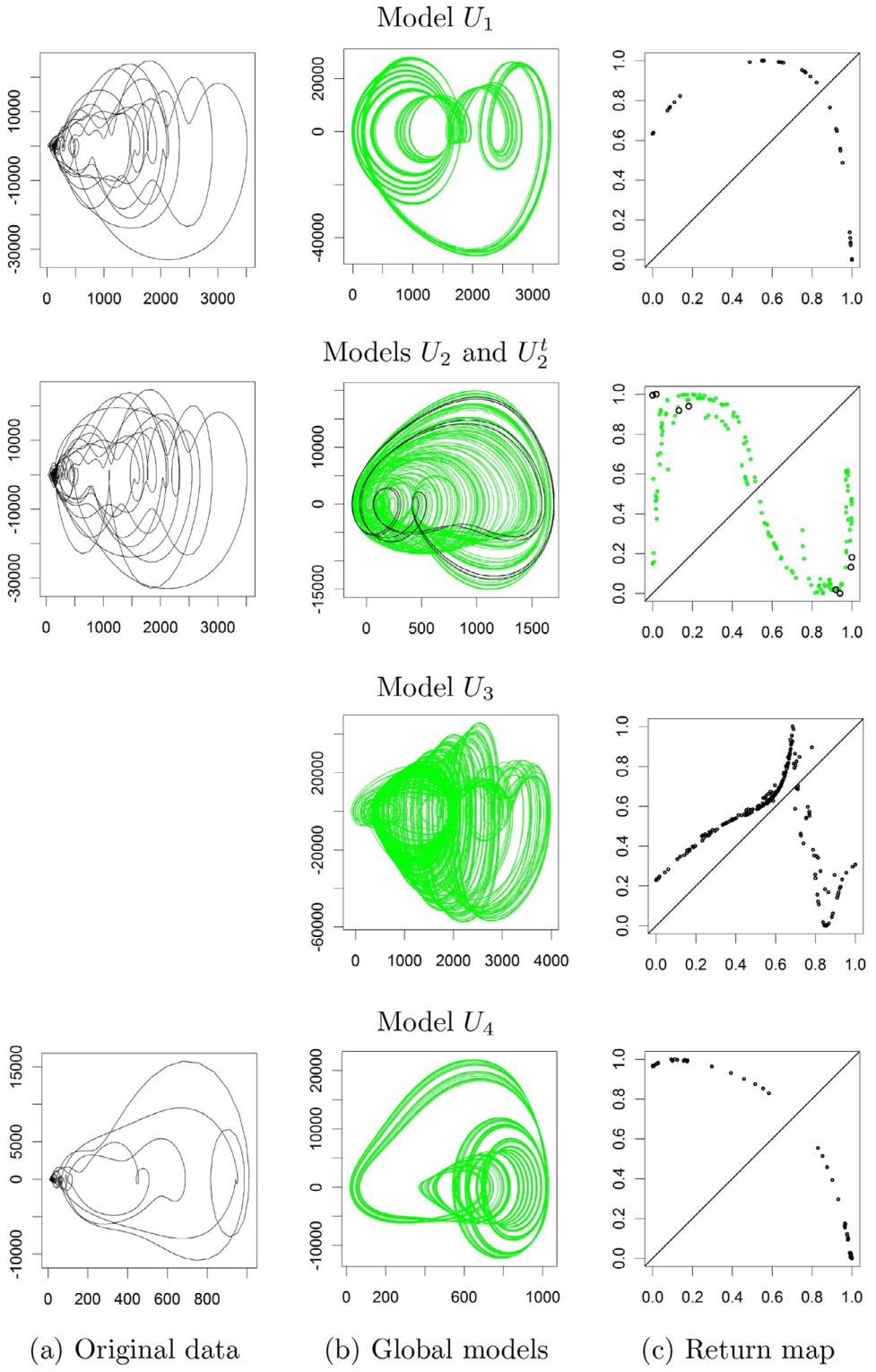

Fig. 3. Phase portraits reconstructed from the original data (1st column) and produced by the global models (2nd column) for models U_1, U_2, U_3 and U_4. For each model, the first-return map to a Poincaré section is also reported (3rd column). For model U_2, which produces initially a period-4 limit cycle (black), the reported attractor (green) was obtained after tuning the parameter values.

cycle than once a new oscillation will have started. Oscillations of small amplitudes during the "non-plague season" (between May–June and October–November) such as the ones observed in 1898 and in 1901 in the original data are obviously retrieved in the models U_1, U_2, U_2^t and U_3 obtained from window B. Such type of intra-seasonal oscillations becomes especially small during window C which probably results from the recommendations of the Advisory Committee aiming to avoid conditions that favor the disease development and its propagation. Such small oscillations remain undetected in model U_4 obtained for this latter window.

4.2. Multivariate modeling

Multivariate modeling (see Section 3.2) was applied to the three variables : x the number of human plague death and y and z the number of captured infected rats *M. decumanus* and *M. rattus*, respectively, with the aim to determine the couplings between the epidemic and the two rat epizooties. Observational records presented in Fig. 2a–c were used for this purpose over the whole window from January 1907 to December 1911 that is included in window C. The corresponding original phase portraits are shown in black in Fig. 4 (model portraits are superimposed in green). The first plane projection (1st column) exhibits a clear hysteresis resulting from the important time delay (equal approximately to 3 weeks) taking place between the epidemic and the epizootic of *M. decumanus*. The second plane projection (2nd column) does not exhibit a salient hysteresis (note that time delay between variables x and z is equal to almost 1.5 week), but rather an almost linear relation between x and z, except for the earlier cycle of the time series (corresponding to 1907 when the higher values of both variables x and z are reached) that exhibits significantly different behaviors. Similarly, the third plane projection (3rd column) does not reveal a salient hysteresis (time delay between y and z, is equal to 1–2 weeks). However, in this latter case, the relation between the two variables appears to be nonlinear rather than linear (a saturation is progressively reached by variable z when y is increasing) except for the earlier cycle of the record for which relation is almost linear.

Several multivariate models were found to be numerically integrable over a long duration (numerical integration were tested for durations 40 times longer than the original 5-year long records. Initial conditions are reported in Table A.1). The model form is a second degree ($q = 2$) polynomial. Only models of concise form (12 parameters or less) were considered and discussed here.

The smaller model obtained is the 10-term model

$$\dot{x} = -0.0976z^2 + 0.045yz - 12.6237\alpha x \tag{3}$$

$$\dot{y} = 0.0107y^2 - 0.0237xy \tag{4}$$

$$\dot{z} = 0.0108z^2 + 1.4512y - 5.912x - 0.0147xz + 0.0041xy, \tag{5}$$

where α is a tuning parameter that equals one by default. This model produces a period-one limit cycle dynamics as shown in Fig. 4 (first raw). By tuning the model parameter values such as $\alpha = 0.598$, it is found that this model can produce a chaotic attractor (see Fig. 5a). Interestingly, the first oscillation observed in the original xz and yz plane projections (2nd and 3rd columns), that was obviously not simulated by model M_0 before its parameterization was tuned, becomes quite well simulated after the tuning (see values of z larger than 400 in M_0^t, 2nd and 3rd panels of Fig. 5). The first return map of the tuned model is smooth and unimodal.

Two other models with a larger number of terms (11-term models) produce more developed dynamics. Their forms are quite similar to the one obtained for model M_0. The first two equations of model M_1 are Eqs. (3) and (4), whereas the third equation is

$$\dot{z} = 0.0213z^2 + 2.0814y - 6.9174x - 0.0255xz + 0.0078xy - 0.0013y^2, \tag{6}$$

one negative term in y^2 is thus added, compared to Eq. (5). Without any tuning, model M_1 produces a chaotic behavior (see Fig. 5b). The resulting attractor has the same structure as the attractor produced by model M_0^t although one of the two branches is less developed. Model M_2 has Eqs. (4) and (5) as second and third equation (the same as model M_0), whereas first Eq. (3) becomes:

$$\dot{x} = -0.1434z^2 + 0.0674yz - 12.7264\alpha x - 0.0025y^2, \tag{7}$$

where the negative term in y^2 is added. By default ($\alpha = 1$), model M_2 produces a period-4 limit cycle (Fig. 4, second line). A chaotic dynamic can be obtained by tuning its parameter values such as $\alpha = 0.9$ (Fig. 5c). The first-return map of this model also corresponds to a two branches chaotic structure. Two 12-term models were also obtained, producing a period-4 limit cycle (Fig. 4c and d). Model M_3 reads

$$\dot{x} = -0.0936z^2 + 0.0431yz - 12.0677\alpha x \tag{8}$$

$$\dot{y} = 0.0103y^2 - 0.0227xy \tag{9}$$

$$\dot{z} = 0.0318z^2 + 1.7263y - 6.6007x - 0.0355xz + 5.967.10^{-3}xy - 0.004x^2 - 7.10^{-4}y^2, \tag{10}$$

that produces a chaotic behavior for $\alpha = 0.945$ (Fig. 5d). Compared to model M_0, only the parameter values of Eqs. (3) and (4) are slightly modified into Eqs. (8) and (9) for variables x and y, and two terms (in y^2 and x^2) are added to Eq. (3) leading to Eq. (10) for variable z. The same two-branches structure for the flow can be deduced from the unimodal smooth first-return map. For model M_4, Eq. (9) for variable y remains the same as model M_3 whereas Eqs. (8) and (10) are changed into

$$\dot{x} = -0.1339\beta z^2 + 0.0627yz - 12.1239\alpha x - 0.0022y^2 \tag{11}$$

$$\dot{z} = 0.0303z^2 + 1.4099y - 6.233x - 0.0339xz + 3.888.10^{-3}xy - 0.0053x^2. \tag{12}$$

Compared to model M_0, model M_4 just has one more term in the equation for x (that is the additional term in y^2) and another one in the equation for z (terms in x^2 as for model M_1).

Model M_4 produces a chaotic behavior for $\beta = 0.975$ (Fig. 5d). It was not possible to get a chaotic dynamics by tuning parameter α as previously done for the other models. The structure of the flow is the same as for models M_0 to M_3.

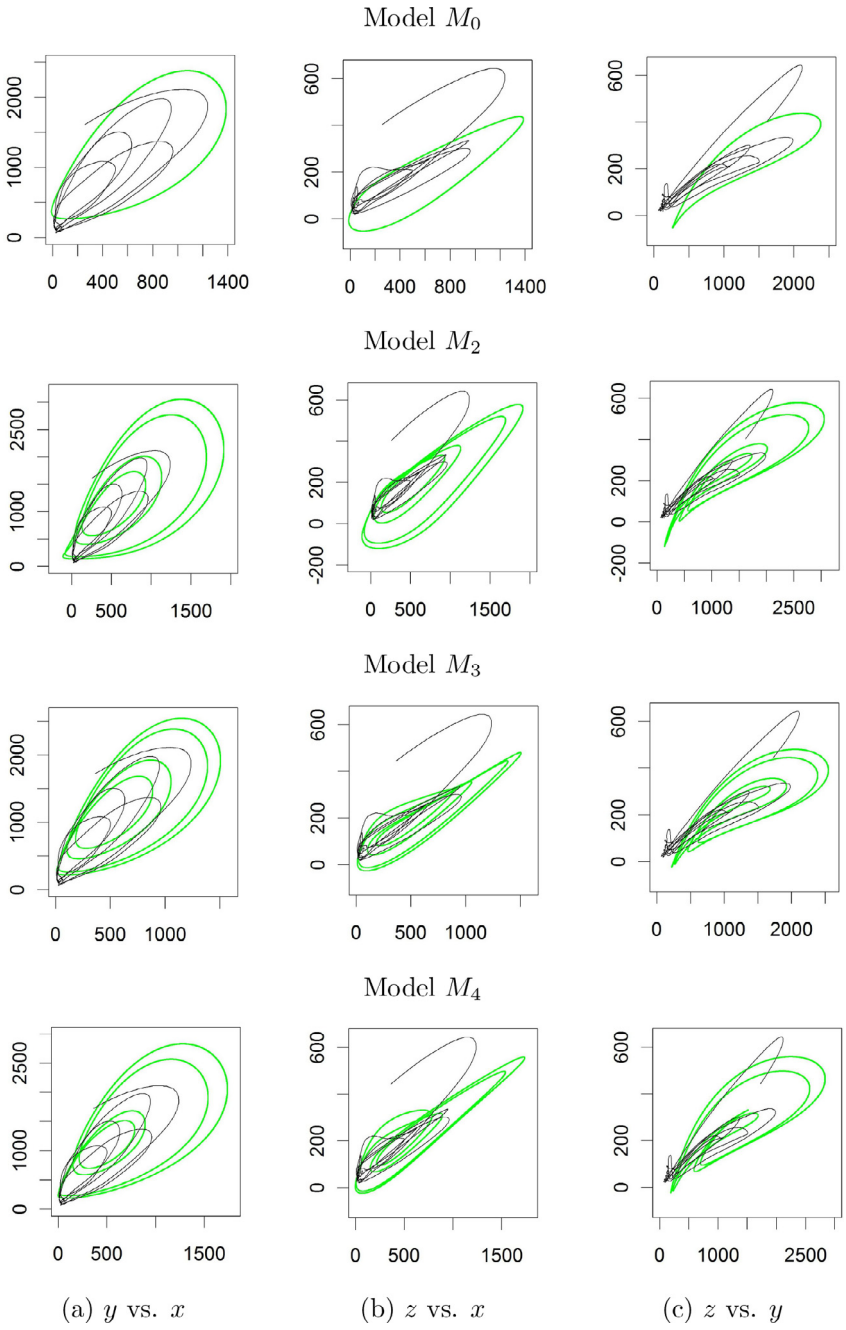

Fig. 4. Different plane projections of the phase portraits for multivariate models M_0, M_2, M_3 and M_4. Original data (in black) are superimposed to data produced by the models (green).

All these multivariate models are built on the same algebraic kernel structure as model M_0; all chaotic attractors are characterized by the same topological structure. Adding polynomial terms to model M_0 mainly permits a better fit to the observed data (for instance, avoiding the negative values of variable y) but does not lead to new behaviors (at least for the parameter values here used, see Fig. 5, 2nd column). The kernel model M_0 can therefore be considered as a proxy of the main processes at work in the observed dynamics.

4.3. Validation

All obtained models (univariate or multivariate) are producing a chaotic attractor (or can produce one after a slight tuning of some parameter values). Such a robustness provides a strong argument for a chaotic dynamics underlying the coupled epizootic–epidemic data. Ideally, validation of such low-dimensional models should be performed based on bifurcation or on topological criteria [20,22]. In practice,

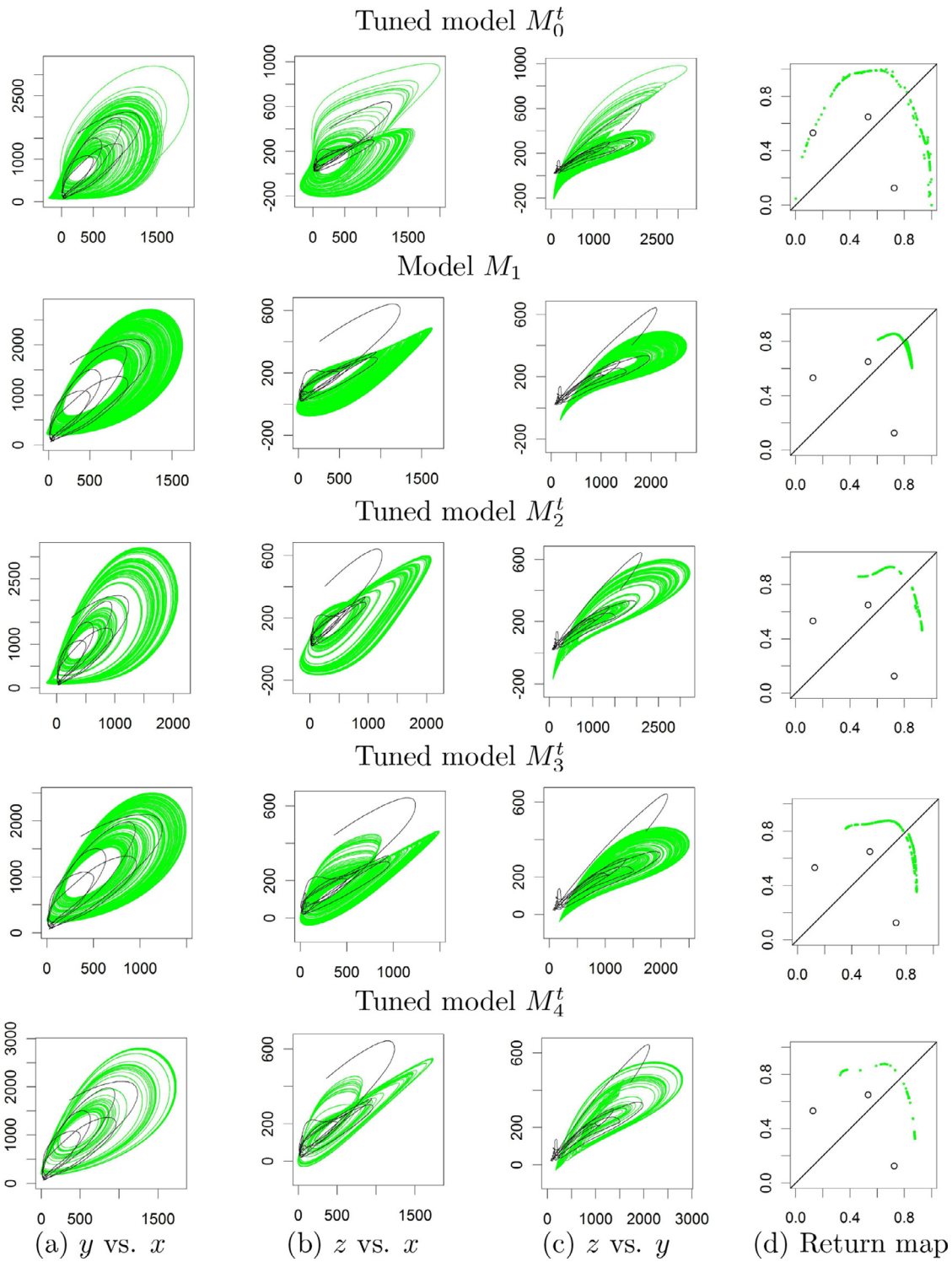

Fig. 5. Different plane projections of the phase portraits for models M_0^t, M_1, M_2^t, M_3^t and M_4^t for parameter values producing chaotic dynamics. Original data (in black) are superimposed to the data produced by the models (green).

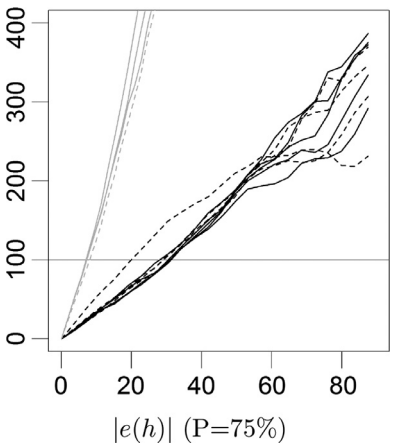

Fig. 6. Third quartile of the absolute error $|e(h)|$ of the number of human plague deaths per half-month as a function of the horizon of prediction h (in day). Models without parameter tuning are plotted as plain lines, and tuned models as dashed lines. Univariate models are in gray, whereas multivariate models are in black. One chosen point $|e(h)|$ of a curve means that, for the corresponding horizon of prediction h, there is probability of 75%, for a forecast, to have an absolute error lower than $|e(h)|$.

such validation would require, for the former, to know the equations of the original system, for the latter, to have sufficiently long (and free of noise) time series. This is not the case here. A more practical model validation is thus performed based on the model forecasting ability. Since the dynamics is chaotic or close to chaos, a strong sensitivity to initial conditions is expected. For this reason, an analysis of the forecasting performances based on a data assimilation or other simpler reinitialization technique should be used. A comparison of the models ability may thus be based on the model horizon of predictability. This can be achieved by estimating the absolute error $|e(h)|$ as a function of the horizon of prediction h, and by comparing the model forecast $\hat{x}(t,h)$ with the recorded data $x(t+h)$ such as

$$|e(h)| = |\hat{x}(t,h) - x(t+h)|, \tag{13}$$

where t is the time at which the forecast is performed and $t+h$ the time to which the forecast is estimated. The third quartile (corresponding to a probability $P = 75\%$) of the distribution of $|e(h)|$ is plotted in Fig. 6 for all the models U_i, U_i^t, M_i and M_i^t (for any i). To estimate the horizon of predictability H_p, the reference threshold error is arbitrarily taken equal to 100 deaths per half-month, which is significantly less that 10% of the maximum peak of plague mortality during the period from 1907 to 1911. Resulting values of H_p are reported in Table 1. The larger error growth for the univariate models than the one for the multivariate models is striking in the present case. Multivariate models are indeed much more robust than the univariate ones, with horizons of predictability H_p near to 4 times longer. It is also interesting to note that, in terms of error growth and horizon of predictability, no systematic difference is observed between tuned models (in dashed lines) and initial models (in plain lines).

Table 2
Average values of the monomials of Eqs. 3, 4 and 5. Terms C_{-x} and C_{+xy} (of average values −1268 and +985, respectively) are grouped in a single term to facilitate the interpretation.

variable x				
terms	A_{+yz}	A_{-z^2}	A_{-x}	
average	+5450.	−2923.	−2707.	
variable y				
terms	B_{+y^2}	B_{-xy}		
average	+5731.	−5695.		
variable z				
terms	C_{-xz}	C_{+y}	C_{+z^2}	C_{-x}+C_{+xy}
average	−845.	+734.	+323.	−282.

5. Discussion

For univariate global models, the algebraic structure cannot be interpreted directly due to their complex algebraic relationship (see [19,45–48]). This is not necessarily the case for multivariate models for which more direct, and thus much simpler couplings may be expected.

All the multivariate models M_i presented in Section 4.2 are built with the same algebraic kernel structure as presented by model M_0; they produce attractors with the same topological properties (see Section 4). For this reason, M_0 can be used as a proxy of the dynamical couplings between variables x, y and z. To analyze the algebraic terms in the kernel model M_0, it is useful to keep in mind that variables x, y and z are – in principle – all positive ($x_i \geq 0$, see Fig. 2). As a consequence, a term contributing to the propagation (resp. to the slow down) of the disease in model M_0 is thus directly identifiable by a positive (negative) sign of its coefficient. Factors and processes that can aggravate the development and propagation of the disease have been mentioned in the introducing Section 1 (transfer of the disease ensured by flea, common places of life for species *M. decumanus* and *M. rattus*, direct proximity between *M. rattus* and man, etc.). Several main processes of negative contribution, that is, slowing down the propagation of the disease, can be identified in the present context, among which (1) the natural immunization [49]; (2) the limitation of the total population of rodents resulting from the sustained monitoring put in place by the Advisory Committee (near to 100,000 rats captured each year from 1906 to 1911); (3) the systematic disinfection and cleansing completed by the Sanitary and Cleansing Department of the City after a case of plague death is declared or detected [11] (p. 733, 735).

To analyze the kernel structure of the multivariate models, let us take Eqs. (3)–(5) of model M_0 one by one in order to analyze its algebraic structure.

Equation for variable x *— The epidemic.* Eq. (3) for variable x is based on three terms: $A_{+yz} = +0.045yz$, $A_{-z^2} = -0.0976z^2$ and $A_{-x} = -12.6237x$ ($\alpha = 1$) whose average contributions are given in a decreasing order of magnitude as $|\overline{A_{+yz}}| < |\overline{A_{-z^2}}| < |\overline{A_{-x}}|$ (see Table 2). The first term $A_{+yz} > 0$ corresponds to the coupled contamination from the two populations of rats (*M. rattus* and *M. decumanus* species), to man. This contribution was one important conclusion of the Advisory Committee. The two other terms are negative feedbacks.

Term A_{-z^2} is interpreted as resulting from the limitation of the total number of rats. It shows the efficiency of the Advisory Committee to slow down the propagation of the disease by the control of the total population of rats. The negative contribution of the last term A_{-x} is proportional to the number of human deaths x. This negative feedback is interpreted as resulting from the disinfection systematically applied by the Advisory Committee once a death is detected. This term may also partly account for immunization.

Equation for variable y — *The* M. decumanus *epizootic.* Eq. (4) for variable y is based on two terms: $B_{+y^2} = +0.0107y^2$ and $B_{-xy} = -0.0237xy$ whose average contributions are very similar in magnitude, $|\overline{B_{+y^2}}| \approx |\overline{B_{-xy}}|$. The positive term B_{+y^2} directly accounts for the self infection of *M. decumanus* specie by itself. Since only one positive term is present, it comes that the propagation of the disease among *M. decumanus* specie is mainly and directly ensured by the number of infected *M. decumanus* inside the specie itself. Since explicitly coupled to variable x, the negative feedback of term B_{-xy} is interpreted as the result of disinfection systematically applied when a case of plague death was found. Although B_{+y^2} and B_{-xy} are similar in average, due to the time delay observed between y and x, the infection will first propagate among *M. decumanus* specie at the beginning of the epizootic (controlled by term in y^2), until human disinfection will become strong enough in response to the number of plague deaths (feedback ensured by terms in x). This observation is consistent with the conclusion of the Advisory Committee that the *M. decumanus* epizootic is the first responsible for the diffusion of plague.

Equation for variable z — *The* M. rattus *epizootic.* Eq. (5) for variable z is made of five terms: $C_{-x} = -5.912x$, $C_{+xy} = 0.0041xy$, $C_{-xz} = -0.0147xz$, $C_{+y} = +1.4512y$ and $C_{+z^2} = 0.0108z^2$ whose average contributions in absolute value are given in a decreasing order. Three terms (C_{+xy}, C_{+y} and C_{+z^2}) are positive, two others (C_{-x} and C_{-xy}) are negative. Term C_{+xy} may be interpreted as a coupled contamination of *M. rattus* by *M. decumanus* and men. However, contamination by men is rarely evoked in the literature and difficult to conciliate with the strongly negative term C_{-x}. Another interpretation can be proposed by grouping these two terms such that

$$C_{-x} + C_{+xy} = 0.0041x(y - 1441.9). \tag{14}$$

This reformulation shows that, for $y < 1441.9$, the effect of disinfection and cleansing is dominant ($C_{-x} + C_{+xy} < 0$). Contrary to this, for $y > 1441.9$, disinfection and cleansing are not enough to reduce the contamination by specie *M. decumanus* which becomes preponderant ($C_{-x} + C_{+xy} > 0$). The interpretation of the three remaining terms appears easier: C_{+y} corresponds to the direct contamination of *M. rattus* by *M. decumanus*, C_{+z^2}, to the self-contamination of *M. rattus*. It is interesting to note that contamination by *M. decumanus* is linear and almost twice in amplitude compared to the *M. rattus* self-contamination ($|C_{+y}|being \approx 2 \times |C_{+z^2}|$). This means that *M. decumanus* epizootic can be considered as responsible for the contamination of *M. rattus* specie (this was one of the conclusions by the Advisory Committee) and that once *M. rattus* is contaminated, the disease can be self-sustained (or at least temporarily maintained) by the *M. rattus* specie itself [11] (p.759). Finally, C_{-xz} is interpreted as the result of disinfection after cases of plague deaths were found (similar interpretation was given to term B_{-xy} in Eq. (4)).

The analysis of the kernel model M_0 is in a good agreement with the main conclusions of the Advisory Committee [11] (see Section 2). It also demonstrates the efficiency of the human actions to slow down the propagation of plague since variable y is almost systematically associated with a strongly negative contribution.

6. Conclusions

The global modeling technique was applied for the first time to the analysis of plague epidemic. Univariate global models were obtained for plague epidemic and multivariate models for the coupling between the epidemic and the epizootic of the two main species of rodents. All these models are either chaotic or close to chaos which brings a direct and strong argument for chaos in plague epidemic systems. Most of the models produce a simple two-branch structure, except two univariate models for which the dynamics is more complex. A statistical analysis of the model forecasting error shows that multivariate models are more robust with horizons of predictability close to four times longer than univariate models.

Models of ordinary differential equations are obtained, for the first time directly from multivariate observational records. Their structure was automatically selected and constrained without any a priori form. These models were used to investigate the couplings between the epidemic and the epizootic of the two main species of rodents *M. decumanus* and *M. rattus* found in Bombay by the end of the 19th century. These models are all built with the same algebraic kernel structure for which a qualitative interpretation is proposed.

The analysis of the multivariate model kernel structure shows that *M. decumanus* specie contributes to sustain the disease among its own specie and to transfer it to *M. rattus* and man. It shows that both species of rats can contribute to the transfer of plague to man. These conclusions are in good agreement with the conclusions reached by the plague Advisory Committee nearly one hundred years ago. Moreover, the analysis shows that, once contaminated, *M. rattus* specie can self-sustained the disease. Finally, the analysis also contributes to demonstrate the efficiency of human action to systematically slow down the propagation of the disease by reducing the number of infected rats and by a systematical cleansing and disinfection of the places where attacks of plague were detected.

The technique used in the present work is quite generic in its formulation, it may be now interestingly applied to other foci of plague or tested to other fields of epidemiology. More generally, it may be used to detect possible couplings at work in any multivariate time series.

Acknowledgments

This work was supported by the french national program *Les Enveloppes Fluides et l'Environnement* LEFE/INSU (MoMu project), by the *IRD-Spirales* program (PamChaos project), by the Institut de Recherche pour le Développement and the Centre National d'Études Spatiales. Discussions with Pr. Christophe Letellier were very encouraging and useful for this project.

Table A.1
Initial conditions for both univariate and multivariate models.

Models	X_1	X_2	X_3
U_1	1278.161	−15178.11	−190389.3
U_2	686.1255	−9467.173	163652.5
U_3	384.7721	−4647.668	20056.898
U_4	897.2336	3896.884	−236101.0
Models	x	y	z
M_0	166.8903	1070.193	138.7208
M_1	895.9957	2391.688	312.7087
M_2	836.9658	1721.620	328.9299
M_3	344.0896	627.7882	101.5058
M_4	161.3367	807.6816	204.2714

Appendix A. Models and initial conditions

A.1. Univariate models

Univariate models U_i (see Table 1) are built on the canonical form given in Eq. 1. Their complete formulation requires the definition of the polynomial approximation $P(X_1, X_2, X_3)$ to function F. For U_1, the polynomial is defined as

$$\begin{aligned} P_1(X_1,X_2,X_3) = {} & 0.033119X_2^2 - 5.185357.10^{-8}X_2^2X_3 \\ & - 1.006865.10^{-6}X_2^3 - 2150.417X_1 \\ & - 0.426848X_1X_2 - 3.924856.10^{-5}X_1X_2^2 \\ & + 3.546094X_1^2 + 3.372379.10^{-6}X_1^2X_3. \end{aligned} \tag{A.1}$$

It is defined as

$$\begin{aligned} P_2(X_1,X_2,X_3) = {} & -424.042518\gamma X_2 + 6.89184.10^{-4}X_2X_3 \\ & + 0.0612896X_2^2 - 1.730567.10^{-6}X_2^3 \\ & - 6022.468886X_1 - 0.0165089X_1X_3 \\ & +0.535031X_1X_2 - 4.979971.10^{-5}X_1X_2^2 \\ & + 4.808114X_1^2 + 8.897116.10^{-6}X_1^2X_3 \\ & - 2.69416.10^{-4}X_1^2X_2, \end{aligned} \tag{A.2}$$

with $\gamma = 1$ for U_2, and with $\gamma = 0.95$ for its tuned version U_2^t. For U_3, the polynomial is defined as

$$\begin{aligned} P_3(X_1,X_2,X_3) = {} & 10.500235X_3 - 3.621546.10^{-5}X_3^2 \\ & - 864.772522X_2 + 0.002437281X_2X_3 \\ & - 1.553974.10^{-9}X_2X_3^2 + 0.061515X_2^2 \\ & - 1.872147.10^{-6}X_2^3 - 5331.507X_1 \\ & - 0.028383X_1X_3 + 1.298926.10^{-8}X_1X_3^2 \\ & + 1.271154X_1X_2 - 1.099917.10^{-6}X_1X_2X_3 \\ & - 5.070679.10^{-5}X_1X_2^2 + 4.974401X_1^2 \\ & + 1.236989.10^{-5}X_1^2X_3 \\ & - 4.856497.10^{-4}X_1^2X_2, \end{aligned} \tag{A.3}$$

and finally, for U_4, it is defined as

$$\begin{aligned} P_4(X_1,X_2,X_3) = {} & 7.818836.10^{-5}X_3^2 - 6.056926.10^{-11}X_3^3 \\ & - 2778.894908X_2 + 0.01513025X_2X_3 \\ & - 1.19701.10^{-8}X_2X_3^2 - 4.090119.10^{-6}X_2^3 \\ & - 8.017016.10^{-8}X_1X_3^2 + 13.452616X_1X_2 \\ & - 2.441398.10^{-5}X_1X_2X_3 - 1.712543X_1^2 \\ & + -0.01555679X_1^2X_2. \end{aligned} \tag{A.4}$$

A.2. Initial conditions

Initial conditions of all models U_i and M_i (see Table 1) are all given in the following Table A.1.

References

[1] Gascuel F, Choisy M, Duplantier J-M, Débarre F, Brouat C. Host resistance, population structure and the long-term persistence of bubonic plague: contributions of a modelling approach in the malagasy focus. PLoS Comput Biol 2013;9(5):e1003039.
[2] Yersin A. La peste bubonique à hong kong. Ann Inst Pasteur 1894;8(11):81–93.
[3] Kermack W, McKendrick A. A contribution to the mathematical theory of epidemics. Bull Math Biol 1927;53(1-2):33–55.
[4] Raggett GF. Modelling the eyam plague. Inst Math Appl 1982;18:221–6.
[5] Keeling M, Gilligan C. Metapopulation dynamics of bubonic plague. Nature 2000;407:903–6.
[6] Monecke S, Monecke H, Monecke J. Modelling the black death. a historical case study and implications for the epidemiology of bubonic plague. Int J Med Microbiol 2009;299(8):582–93.
[7] Bacaër N. The model of kermack and mckendrick for the plague epidemic in bombay and the type reproduction number with seasonality. J Math Biol 2012;64(3):403–22.
[8] Boire N, Riedel VAA, Parrish NM, Riedel S. Lessons learned from historic plague epidemics: the relevance of an ancient disease in modern times. J Anc Dis Prevent Rem 2014;2(114).
[9] Andrianaivoarimanana V, Kreppel K, Elissa N, Duplantier J-M, Carniel E, Rahalison L, et al. Understanding the persistence of plague foci in madagascar. PloS Negl Trop Dis 2013;7(11):e2382.
[10] Andrianaivoarimanana V, Telfer S, Rajerison M, Ranjalahy MA, Andriamiarimanana F, Rahaingosoamamitiana C, et al. Immune responses to plague infection in wild rattus rattus, in madagascar: a role in foci persistence? PloS One 2012;7(6):e38630.
[11] Plague Research Commission. The epidemiological observations made by the commission in bombay city. J Hyg 1907;7:724–98.
[12] McCoy GW. Plague among ground squirrels in america. J Hyg 1910;10(4):589–601.
[13] Johnson TL, Cully Jr JF. Spread of plague among black-tailed prairie dogs is associated with colony spatial characteristics. J Wildl Manag 2011;75(2):357–68.
[14] Hufthammer AK, Walløe L. Rats cannot have been intermediate hosts for yersinia pestis during medieval plague epidemics in northern europe. J Archaeol Sci 2013;40:1752–9.
[15] Tollenaere C, Brouat C, Duplantier J-M, Rahalison L, Rahelinirina S, Pascal M, et al. Phylogeography of the introduced species rattus rattus in the western indian ocean, with special emphasis on the colonization history of madagascar. J Biogeogr 2010;37(3):398–410.
[16] Hirst LF. Rat-flea surveys and their use as a guide to plague preventive measures. Trans R Soc Trop Med Hyg 1927;21(2):87–108.
[17] Klein J-M, Hébrard G, Suor K. Etude écologique sur les puces de rats commensaux de l'homme et en particulier sur xenopsylla cheopis (roths.), 1903 (siphonaptera), dans la région de phnom-penh (cambodge). Cahiers ORSTOM Série Entomol Méd Parasitol 1973;11(1):57–73.
[18] Liston W. Plague, rats and fleas. Indian Med Gaz 1905;40:43.
[19] Gouesbet G, Letellier C. Global vector-field reconstruction by using a multivariate polynomial l_2 approximation on nets. Phys Rev E 1994;49(6):4955.
[20] Aguirre LA, Billings SA. Dynamical effects of overparametrization in nonlinear models. Physica D: Nonlinear Phenom 1995;80(1):26–40.
[21] Aguirre LA, Furtado EC. Building dynamical models from data and prior knowledge: the case of the first period-doubling bifurcation. Phys Rev E 2007;76(4):046219.
[22] Letellier C, Sceller LL, Dutertre P, Gouesbet G, Fei Z, Hudson J. Topological characterization and global vector field reconstruction of an experimental electrochemical system. J Phys Chem 1995;99(18):7016–27.
[23] Letellier C, Aguirre L, Maquet J, Gilmore R. Evidence for low dimensional chaos in sunspot cycles. Astron Astrophys 2006;449(1):379–87.
[24] Maquet J, Letellier C, Aguirre LA. Global models from the canadian lynx cycles as a direct evidence for chaos in real ecosystems. J Math Biol 2007;55(1):21–39.

[25] Mangiarotti S, Drapeau L, Letellier C. Two chaotic global models for cereal crops cycles observed from satellite in northern morocco. Chaos: Interdiscip J Nonlinear Sci 2014;24(2):023130.
[26] Mangiarotti S. Modélisation globale et caractérisation topologique de dynamiques environnementales: de l'analyse des enveloppes fluides et du couvert de surface de la terre à la caractérisation topolodynamique du chaos. Habilitation to direct Researches, Université de Toulouse 3 2014.
[27] The reported appearance of plague in bombay, Br Med J 1886 (1896 Oct 3) 966.
[28] Gatacre W.F. Report: Bubonic plague in bombay. 1896–1897.
[29] Ogata M. Ueber die pestepidemie in formosa. Centralbl f Bakteriol 1897;21:774.
[30] Simond P-L. La propagation de la peste. Annales d'hygiène et de médecine coloniale 1899;02:80–98.
[31] Hankin E. On the epidemiology of plague. J Hyg 1905;5(01):48–83.
[32] Verjbitski D. Xxvi. the part played by insects in the epidemiology of plague (translation of a thesis presented for the degree of doctor of medicine of the university of st petersburg in 1904). J Hyg 1908;8(02):162–208.
[33] Pollitzer R. Plague. Geneva: WHO; 1954. p. 409–82.
[34] Yu H-L, Christakos G. Spatiotemporal modelling and mapping of the bubonic plague epidemic in india. Int J Health Geogr 2006;5(1):12.
[35] Indian Plague Commission, et al. Reports on plague investigation in india, xxxi: On the seasonal prevalence of plague in india. J Hyg 1908;8:266–301.
[36] The advisory committee, reports on plague investigation in india, xlix: Statistics of the occurrence of plague in man and rats in bombay, 1907–1911, J Hyg 1912;XII:220–226
[37] Numerous other Reports on plague investigation in India were published in the Journal of Hygienne between 1906 and 1917. These can be found at http://www.ncbi.nlm.nih.gov/pmc/journals/326/.
[38] Seal SC. Epidemiological studies of plague in india, 2. the changing pattern of rodents and fleas in calcutta and other cities. Bull Wld Hlth Org 1960;23:293–300.
[39] Seal SC. Epidemiological studies of plague in india, 1. the present position. Bull Wld Hlth Org 1969;23:283–92.
[40] Condon JK. The bombay plague: being a history of the progress of plague in the bombay presidency from september 1896 to june 1899 (Appendix A. Northern Division). Printed at the Education Society's Steam Press; 1900.
[41] Dennison C. India: bombay – plague, cholera, smallpox, and smallpox in 1909. Public Health Rep (1896–1970) 1910;25(47):1731–3.
[42] Savitzky A, Golay MJ. Smoothing and differentiation of data by simplified least squares procedures. Anal Chem 1964;36(8):1627–39.
[43] Mangiarotti S, Coudret R, Drapeau L, Jarlan L. Polynomial search and global modeling: two algorithms for modeling chaos. Phys Rev E 2012;86(4):046205.
[44] Letellier C, Ringuet E, Maheu J, Maquet J, Gouesbet G. Global vector field reconstruction of chaotic attractors from one unstable periodic orbit. Entropie 1997;202/203:147–53.
[45] Gouesbet G. Reconstruction of the vector fields of continuous dynamical systems from numerical scalar time series. Phys Rev A 1991;43(10):5321.
[46] Gouesbet G. Reconstruction of vector fields: the case of the lorenz system. Phys Rev A 1992;46(4):1784.
[47] Letellier C, Aguirre LA, Maquet J. Relation between observability and differential embeddings for nonlinear dynamics. Phys Rev E 2005;71(6):066213.
[48] Lainscsek C, Letellier C, Gorodnitsky I. Global modeling of the rössler system from the z-variable. Phys Lett A 2003;314(5):409–27.
[49] The advisory committee, reports on plague investigation in india, vi. a note on the immunity of bombay rats to subcutaneous injection of plague cultures, J Hyg 1906;VI:506–508